

UCSF

UC San Francisco Previously Published Works

Title

Evaluation of the distribution and progression of intraluminal thrombus in abdominal aortic aneurysms using high-resolution MRI

Permalink

<https://escholarship.org/uc/item/1q720731>

Journal

Journal of Magnetic Resonance Imaging, 50(3)

ISSN

1053-1807

Authors

Zhu, Chengcheng
Leach, Joseph R
Tian, Bing
[et al.](#)

Publication Date

2019-09-01

DOI

10.1002/jmri.26676

Peer reviewed



Published in final edited form as:

J Magn Reson Imaging. 2019 September ; 50(3): 994–1001. doi:10.1002/jmri.26676.

Evaluation of the Distribution and Progression of Intraluminal Thrombus in Abdominal Aortic Aneurysms Using High-Resolution MRI

Chengcheng Zhu, PhD^{1,*}, Joseph R. Leach, PhD, MD¹, Bing Tian, MD², Lizhen Cao, MD¹, Zhaoying Wen, MD^{1,3}, Yan Wang, PhD¹, Xinke Liu, MD^{1,4}, Qi Liu, MD², Jianping Lu, MD^{2,*}, David Saloner, PhD¹, Michael D. Hope, MD¹

¹Department of Radiology and Biomedical Imaging, UCSF, San Francisco, California, USA;

²Department of Radiology, Changhai Hospital, Shanghai, China;

³Department of Radiology, Beijing Anzhen Hospital, Capital Medical University, Beijing Institute of Heart, Lung and Blood Vessel Disease, Beijing, China;

⁴Department of Interventional Neuroradiology, Beijing Neurosurgical Institute and Beijing Tiantan Hospital, Capital Medical University, Beijing, China

Abstract

Background: Intraluminal thrombus (ILT) signal intensity on MRI has been studied as a potential marker of abdominal aortic aneurysm (AAA) progression.

Purpose: 1) To characterize the relationship between ILT signal intensity and AAA diameter; 2) to evaluate ILT change over time; and 3) to assess the relationship between ILT features and AAA growth.

Study Type: Prospective.

Subjects: Eighty AAA patients were imaged, and a subset ($n = 41$) were followed with repeated MRI for 16 ± 9 months.

Field Strength/Sequence: 3D black-blood fast-spin-echo sequence at 3 T.

Assessment: ILT was designated as “bright” if the signal was greater than 1.2 times that of adjacent psoas muscle. AAAs were divided into three groups based on ILT: Type 1: bright ILT; Type 2: isointense ILT; Type 3: no ILT. During follow-up, an active ILT change was defined as new ILT formation or an increase in ILT signal intensity to bright; stable ILT was defined as no change in ILT type or ILT became isointense from bright previously.

Statistical Tests: Shapiro-Wilk test; Mann-Whitney *U*-test; Fisher’s exact test; Kruskal-Wallis test; Spearman’s *r*; intraclass correlation coefficient (ICC), Cohen’s kappa.

*Address reprint requests to: C.Z., Department of Radiology and Biomedical Imaging, 4150 Clement St., San Francisco, CA 94121. chengcheng.zhu@ucsf.edu or J.L., Department of Radiology, Changhai Hospital, 168 Changhai Road, Shanghai, 200433, China. cjr.lujianping@vip.163.com.

Additional supporting information may be found in the online version of this article

Results: AAAs with Type 1 ILT were larger than those with Types 2 and 3 ILT (5.1 ± 1.1 cm, 4.4 ± 0.9 cm, 4.2 ± 0.8 cm, $P = 0.008$). The growth rate of AAAs with Type 1 ILT was significantly greater than that of AAAs with Types 2 and 3 ILT (2.6 ± 2.5 , 0.6 ± 1.3 , 1.5 ± 0.6 mm/year, $P = 0.01$). During follow-up, AAAs with active ILT changes had a 3-fold increased growth rate compared with AAAs with stable ILT (3.6 ± 3.0 mm/year vs. 1.2 ± 1.5 mm/year, $P = 0.008$).

Data Conclusion: AAAs with bright ILT are larger in diameter and grow faster. Active ILT change is associated with faster AAA growth. Black-blood MRI can characterize ILT features and monitor their change over time, which may provide new insights into AAA risk assessment.

THE RUPTURE RISK of abdominal aortic aneurysms (AAAs) increases with aneurysm diameter.¹ Patients with AAAs >5.5 cm typically undergo elective repair because this is the threshold when the risk of AAA rupture exceeds the risk of repair.¹ While easy to understand and practical for clinical use, AAA risk stratification by maximum diameter is limited: a considerable number of smaller AAAs will rupture.¹ Other aneurysm features including diameter expansion rate, biomechanical vessel wall stress, inflammation, and intraluminal thrombus (ILT) have been studied in an effort to improve risk stratification for progressive AAA disease.²⁻⁵

ILT is a common feature in AAAs and has been studied as a potential marker of progressive AAA disease. ILT size and wall coverage have been related to AAA growth.² Thick ILT can induce localized hypoxia and inflammation and weaken the underlying arterial wall,⁶ and could play a role in the rupture of smaller aneurysms.⁷ Additionally, ILT growth has been associated with rupture.⁸ Magnetic resonance imaging (MRI) can show not only the size and location of ILT, but also its unique signal characteristics. AAAs with high signal intensity intraluminal thrombus on T₁-weighted MRI have been reported to grow 3 times faster (in cross-sectional area) than those without high signal ILT.⁹

Despite these reports connecting ILT with AAA progression, little is known about the natural history of ILT and the distribution of different subtypes of ILT across AAA diameters. The goal of this study was to use high-resolution black-blood MRI: 1) to characterize the relationship between ILT signal intensity and AAA diameters; 2) to evaluate ILT changes over time; and 3) to assess the relationship between ILT features and AAA growth.

We hypothesize that AAAs with different ILT subtypes are different in size, and that certain ILT subtypes or changes are associated with AAA growth.

Materials and Methods

Study Population

Patient studies were conducted following human subject approval by the Institutional Review Board (IRB) of the University of California San Francisco or the Ethics Committee of Changhai Hospital in China. All subjects provided informed written consent for study participation. This was a prospective, cross-sectional study with a subset who had longitudinal assessments.

From August 2014 to April 2018, patients with AAA disease (>3 cm in diameter as identified on either ultrasound or computed tomography [CT]) were recruited at two centers, one in the United States (University of California San Francisco), the other in China (Changhai Hospital, Shanghai). All patients underwent a baseline high-resolution MRI, and a subset were followed by MRI. The follow-up criteria followed the clinical guidelines for monitoring of patients with AAA.¹ Patients with symptomatic or large (>5.5 cm) AAAs were selected for intervention and had no subsequent MRI follow-up. Patients with asymptomatic AAAs smaller than the intervention threshold (5.5 cm) were routinely followed with the higher-resolution MRI protocol every 6–12 months.

Scanning Protocols

MRI scans were performed on Siemens (Erlangen, Germany) Skyra 3 T scanners. A 3D black-blood MRI sequence (blood-suppressed T₁-weighted fast-spin-echo with variable flip angle train, DANTE-SPACE^{10,11}) was used to image the 3D AAA geometry and the ILT composition. Images were acquired in the coronal plane with 56 slices and 1.3 mm slice thickness. Scanning parameters: repetition time / echo time (TR/TE): 800/20 msec, 32 × 32 cm field of view, 256 × 256 matrix, 1.3 mm in-plane resolution, echo train length 60, scan time 7 minutes and 10 seconds. The DANTE module suppresses the signal of flowing blood, allowing good visualization of the ILT/wall. This technique has been validated against CTA.

¹¹ Patients also had contrast-enhanced MR angiography (MRA) or CTA scans as references.

Image Analysis

Two radiologists (L.C. and Z.W. with 9 years' and 11 years' experience in evaluating AAAs) independently measured the maximal AAA diameter using multiplanar reconstruction. ILT was designated as bright if its signal intensity on black-blood MRI was greater than 1.2 times that of adjacent psoas muscle,⁹ and ILT was designated as isointense when the ILT/psoas signal intensity ratio was lower than 1.2. AAAs were divided into three groups based on ILT subtypes independently by the two radiologists: Type 1: presence of bright ILT; Type 2: isointense ILT; Type 3: no ILT. Sample images of the three AAA types are shown in Fig. 1.

Two radiologists independently classified the ILT for each imaging study, with any disagreements solved by discussion and consensus. At the location of maximum AAA diameter, the ILT thickness and area were recorded. The lumen and outer wall boundaries of AAA were automatically segmented using a previously developed level-set method (Fig. 2a).¹² Another experienced reviewer checked the segmentation results and manually corrected the contours when the automatic segmentation method had errors. The volume of ILT and of the entire AAA were recorded. The signal intensity of the entire ILT volume was recorded, and the ILT-to-psoas signal intensity ratio was calculated. The heterogeneity of ILT signal was calculated as the heterogeneity index = SD/mean of ILT signal (Fig. 2b).

Patient information including age, sex, smoking status, and comorbid hypertension, diabetes, and coronary artery disease was recorded, and the relationship between ILT type and AAA diameter/traditional risk factors was analyzed.

Patients with greater than 6 months follow-up were included in the longitudinal analysis. The annual growth rate of an AAA was calculated as (the maximal diameter of the AAA - the baseline diameter) / follow-up duration (in years). During follow-up, active ILT change was defined as new ILT formation or ILT becoming bright (either ILT changed from totally iso-intense to bright, or bright ILT increased by more than 25% of the overall ILT area); stable ILT was defined as no change in ILT type or ILT became darker. The relationship between ILT features and AAA growth was evaluated.

Statistical Analysis

Continuous data were summarized using the mean \pm standard deviation or median (interquartile range). Categorical data were expressed as counts or percentages. As the subgroups often had a sample size around 20 or smaller, nonparametric statistical analysis was used. Continuous data were compared using a Mann-Whitney *U*-test. Categorical variables were analyzed using Fisher's exact test. Growth rates of multiple groups were compared using Kruskal-Wallis test. Spearman's *r* was used to describe the correlation between measured parameters and AAA growth rate. The reproducibility of measurements was evaluated by the intraclass correlation coefficient (ICC) and the agreement of ILT type classification was evaluated by Cohen's kappa. $P < 0.05$ was considered statistically significant. All *P*-values were two-sided. Post-hoc sample size was calculated using 0.8 power and 0.05 significance as described in a previous publication.¹³ GraphPad prism 7 (GraphPad Software, San Diego, CA) and R Statistics (v. 3.1.3, www.r-project.org) were used for data analysis.

Results

A total of 85 patients met the inclusion criteria, and five patients were excluded due to insufficient image quality (exclusion rate of 6%). Images from two patients showed severe motion artifacts and images from three patients had low signal-to-noise ratio (SNR). The low SNR was attributed to large patient size and resultant B₁+ inhomogeneity. Fast-spin-echo sequences used 90° excitation and 180° refocusing pulses, and nonperfect flip angles deep in the abdomen result in signal loss. In total, 80 patients (five female, age 72 ± 7 years) were included in this study. In all, 59 patients were recruited at University of California San Francisco and 21 patients were recruited at Changhai Hospital, Shanghai. The average AAA diameter was 4.6 ± 0.9 cm at baseline. Demographic data are listed in Table 1.

ILT Types, AAA Diameter, and Traditional Risk Factors

The diameters of AAAs with different ILT types were different (Type 1: 5.1 ± 1.1 cm, Type 2: 4.4 ± 0.9 cm, Type 3: 4.2 ± 0.8 cm, $P = 0.008$), as shown in Fig. 3. AAAs with Type 1 ILT were larger than AAAs with ILT Types 2 and 3 ($P = 0.04$ and 0.003). No significant difference was found between AAAs with Type 2 and Type 3 ILT ($P = 0.49$). There was a significantly larger percentage of bright ILT presentation in larger AAAs (diameter > 5.5 cm) than in smaller AAAs (diameter < 5.5 cm) ($11/13 = 84.6\%$ vs. $28/67 = 41.8\%$, $P = 0.005$).

As shown in Table 1, ILT types were not associated with traditional risk factors ($P > 0.05$).

Longitudinal Analysis

Patients recruited at the center in China ($n = 21$) had no follow-up data available because they were either outpatients or underwent intervention shortly after imaging. Of the remaining 59 patients who were recruited at the US center, 18 patients were excluded from the longitudinal analysis because: 1) their AAAs were symptomatic or large (>5.5 cm) at baseline imaging and they were offered intervention without further MRI follow-up ($n = 8$); 2) they were lost to follow-up ($n = 2$); 3) image quality was insufficient ($n = 3$); 4) the follow-up interval was too short, <6 months ($n = 3$); or 5) they were recently recruited to the study and had not yet met the time interval criterion for follow-up imaging ($n = 2$).

Forty-one patients were ultimately included for longitudinal analysis with an average follow-up duration of 16 ± 9 months. Twenty-seven patients received one follow-up study, and 14 patients received two or more follow-up studies. There was no significant difference in patient demographic data between the whole group and the subset follow-up group (Supplemental Table 1). The size of AAA in the whole group was larger than the size in the subset (4.6 ± 0.9 cm vs. 4.2 ± 0.8 cm, $P = 0.02$), as patients with AAAs larger than 5.5 cm were immediately offered treatment.

During follow-up, AAAs grew from 4.2 ± 0.8 cm to 4.4 ± 0.9 cm, with an annual growth rate of 1.6 ± 1.9 mm/year (range -0.8 mm/year to 10.1 mm/year). At baseline, the numbers of AAAs with different ILT types were: $n = 13$ for Type 1, $n = 9$ for Type 2, $n = 19$ for Type 3. As shown in Fig. 4, AAA growth rate was significantly different among these three groups by Kruskal-Wallis test (Type 1: 2.6 ± 2.5 , Type 2: 0.6 ± 1.3 , Type 3: 1.5 ± 1.6 mm/year, $P = 0.01$). P values for each pair were also significant (1 vs. 2: 0.009 , 1 vs. 3: 0.04 , 2 vs. 3: 0.05). In this subgroup of patients with follow-up, the baseline diameters of AAAs with the three different ILT types were not significantly different ($4.5 \pm 0.8, 4.1 \pm 0.8, 4.1 \pm 0.8$ cm, $P = 0.31$).

During follow-up, the majority of ILT were stable ($34/41 = 82.9\%$, no change in 31, darker in 3). Seven (17.1%) AAAs had active ILT changes: new ILT formation ($n = 3$) or an existing ILT became bright ($n = 4$). As shown in Fig. 5, AAAs with active ILT changes had a 3-fold increased growth rate compared with the AAAs with stable ILT (3.6 ± 3.0 mm/year vs. 1.2 ± 1.3 mm/year, $P = 0.008$), while their baseline diameters were comparable (4.6 ± 0.9 cm vs. 4.1 ± 0.8 cm, $P = 0.35$).

In the stable ILT group ($n = 34$), there were 10 stable bright ILTs, and five stable isointense ILTs. The growth rate of stable bright ILT was comparable to that of stable isointense ILT (0.7 ± 1.2 mm/year vs. 1.0 ± 1.4 mm/year, $P = 0.53$). Actively changing ILT tended to have a larger growth rate than bright stable ILT (3.6 ± 3.0 mm/year vs. 0.7 ± 1.2 , $P = 0.07$).

AAA growth rate was moderately associated with baseline diameter (Spearman's $r = 0.44$, $P = 0.004$). ILT area change was not associated with AAA growth ($r = 0.42$, $P = 0.06$). In patients with ILT ($n = 22$), the AAA growth rate was moderately associated with ILT thickness change ($r = 0.53$, $P = 0.02$) and baseline ILT volume ($r = 0.43$, $P = 0.05$). ILT volume changed during follow-up from 28.3 ± 27.8 ml to 31.8 ± 29.9 ml, while the entire AAA volume changed from 46.5 ± 49.9 ml to 51.4 ± 41.9 ml. ILT volume change was not

associated with overall AAA growth ($r = 0.09$, $P = 0.70$). Baseline ILT to psoas signal intensity ratio was not associated with growth ($r = -0.06$, $P = 0.78$), but the change in signal intensity ratio over time tended to moderately correlate with growth, with borderline significance ($r = 0.41$, $P = 0.06$, Fig. 6). The ILT heterogeneity index changed from 0.31 ± 0.07 to 0.32 ± 0.07 , and neither the baseline index nor its change over time were associated with AAA growth ($r = 0.27$, $P = 0.24$; $r = 0.005$, $P = 0.98$).

Example cases are shown in Figs. 7 and 8.

Measurement Reproducibility

There was good agreement for ILT type classifications between two radiologists, with a Cohen's kappa of 0.85. There were four disagreements between the two reviewers. Three were disagreements between bright and isointense ILT, due to a borderline ILT-to-muscle signal intensity ratio. Consensus was made after several more measurements by the two reviewers together. One disagreement was between isointense ILT and no ILT, due to a very thin ILT that one reviewer thought could be vessel wall. The final consensus was ILT, as its thickness was >5 mm.

The interobserver reproducibility was excellent for measurements of maximal diameter (ICC = 0.986), ILT thickness (ICC = 0.942), and ILT area (ICC = 0.965).

Post-Hoc Power Analysis for Sample Size

The measurement error (SD of the difference of two reviewer's measurement) of AAA diameter was 1.2 mm, while the average AAA growth was 2.1 mm, so coherence of variance (CV) was $1.2/2.1 = 57\%$. The differences of growth rate among AAA with different ILT types were 0.9 mm/year, 1.1 mm/year, and 2 mm/year. The growth rate difference between AAAs with active vs. stable ILT was 2.4 mm. The overall average AAA growth rate was 1.6 mm/year. The calculated sample size to detect 0.9 mm change ($0.9/1.6 = 56\%$ change) was 33, and 1.1 mm change ($1.1/1.6 = 69\%$ change) was 22, and 2.0 mm change ($2.0/1.6 = 125\%$) was 7 and 2.4 mm change ($2.4/1.6 = 150\%$ change) was 5.

Discussion

In this study we evaluated the maximal aneurysm diameter among AAAs with different ILT types. We found AAAs with bright ILT are larger and grow faster than AAAs without bright ILT. This is also the first study to use high-resolution black-blood MRI to report ILT signal intensity change over time. We found that active ILT change was associated with a 3-fold faster AAA growth when compared with cases where ILT was stable. Noncontrast black-blood MRI had advantages over previous contrast-enhanced gradient-echo sequences, as it did not require gadolinium (Gd) contrast and provided higher resolution and a shorter scan time. Aneurysm growth rate was correlated with baseline aneurysm diameter in our study, reinforcing what has been shown previously.^{14,15}

Our results demonstrate that bright ILT is identified with increasing frequency in larger aneurysms, possibly representing less-organized degraded thrombus, hemorrhagic material, or more recently layered thrombus, depending on position between the lumen and vessel

wall. As AAAs increase in size, continued deposition of fresh thrombus, intrathrombus fibrinolysis and red cell lysis, and limited penetration of circulating erythrocytes lead to blood products of varying age and differences in fibrin content and structure throughout the ILT thickness.¹⁶ AAAs without ILT were smaller in size, which agreed with previous studies that correlated ILT volume with aneurysm diameter.^{17,18} We did not observe a relationship between ILT composition and traditional AAA progression risk factors.

We found that the bright ILT was associated with relatively more rapid AAA growth, which agrees with a previous study.⁹ Our study provides additional evidence that ILT composition may be a potential marker for AAA expansion, with several advantages over the previous study. First, our study achieved longer follow-up duration (~16 months in our study vs. ~6 months in that study). Second, we used aneurysm diameter change, while the prior study used maximal cross-sectional area change. Currently, aneurysm expansion is clinically assessed by an interval change in maximum diameter, while the utility of area change has not been validated in clinical studies. Third, we used a 3D high-resolution noncontrast black-blood MRI technique at 3 T, while the prior study used traditional 2D gradient recalled echo (GRE) sequence at 1.5 T with contrast. Our noncontrast technique is feasible for patients with renal insufficiency, avoids the concern of Gd deposition in the brain, and has a shorter scan time (7 min vs. 9.5 min plus contrast injection) and higher resolution than the previous GRE method.

There was little change in ILT subtype during short-term follow-up (<2 years). However, when new ILT was deposited or existing ILT became brighter, the growth rate increased by 3-fold. This suggests that *increasing* ILT signal intensity may be related to more rapid aneurysm expansion, and that a common pathway may guide the evolution of both the presence and signal characteristics of ILT and the morphology of the aneurysmal vessel wall. A large body of work reveals the interconnectedness of biochemomechanical factors that mediate platelet activation, aggregation, and adherence in thrombus deposition,^{19,20} vessel wall remodeling, and mechanical stability,¹⁶ and the complex biologic and mechanical interactions at the thrombus/wall interface.^{6,16,21,22} One of the major aims of this study was to understand the morphology and composition changes of ILT during AAA progression. However, it is still premature to evaluate the prognostic value of monitoring ILT changes over time for predicting future AAA growth. Our study is limited by a small sample size and many of the patients did not have more than one follow-up study. Our initial data highlights the importance of performing a larger cohort study with longer follow-up duration to evaluate the true prognostic value of monitoring ILT composition changes.

In our cohort, AAA expansion was related to baseline ILT type, but is not specifically related to the ILT-to-muscle signal intensity ratio. The measurement of the ILT/muscle signal intensity ratio was an average over the whole ILT volume, which may not fully represent the composition of the ILT. For example, focally bright ILT can be present without increasing the overall ratio significantly. The ILT-to-muscle signal intensity ratio increase tended to correlate with faster AAA growth, with borderline significance, which agreed with the qualitative analysis that active ILT promoted faster growth. We did not observe any relationship between the heterogeneity of ILT signal or its change over time and AAA growth. The heterogeneity index changed very little over time, reflected in most ILTs

qualifying as “stable.” Previous studies suggest ILT thickness and area are associated with AAA growth rate.^{2,23} We found no association between ILT area change and AAA growth, but a moderate correlation between ILT thickness change and growth. As measurements were made at the cross-section of the maximum AAA diameter, ILT area is more representative of ILT mass and correlation between AAA growth and ILT thickness change could represent a redistribution of thrombus. As only a subset of AAAs in our longitudinal analysis had ILT (22 of 41 patients), a larger cohort is needed to confirm our findings.

Although the relatively long period of follow-up in our study gives weight to growth data, there are several limitations. First, only half of our study population had sufficient follow-up and no follow-up data were available at the Chinese center. The sample size in this study was either more than sufficient or close to sufficient to offer major conclusions (bright ILT grew faster than isointense ILT, and active ILT grew faster than stable ILT). Future larger-scale studies and multivariable analysis should be performed to confirm whether ILT composition is an independent predictor of AAA growth, and ultimately rupture risk. Such a larger-scale study can also address which ILT feature is most important (bright ILT, active ILT, or ILT heterogeneity). Second, no gross or histologic validation of ILT macrostructure and biochemical composition was performed in this cohort; such validation could strengthen our hypotheses regarding the etiology of signal changes, and shed light on the underlying biochemomechanics that govern the complex and related evolution of aortic aneurysms and intraluminal thrombus. Third, although we provided both qualitative and quantitative descriptions of ILT signal and thrombus burden, future work including quantification of 3D morphology and texture could improve the characterization of ILT from the rich 3D datasets.^{12,24} Future work may also incorporate more advanced imaging methods including MRI and PET/CT markers of inflammation, providing a more comprehensive evaluation of both ILT and the underlying vessel wall.^{25–28} Additionally, different ILT signal intensity may correlate with different mechanical characteristics,^{9,29} which could better inform computational modeling of AAA mechanics.

In conclusion, bright ILT is more common in large AAAs and predicts faster AAA growth. Active ILT change is also associated with faster AAA growth. High-resolution black-blood MRI can characterize ILT composition and monitor its change over time, which may provide new insights into AAA risk assessment.

Supplementary Material

Refer to Web version on PubMed Central for supplementary material.

Acknowledgment

Contract grant sponsor: National Institutes of Health (NIH); Contract grant numbers: R01HL114118, R01HL123759, K99HL136883.

References

1. LeFevre ML, Force USPST. Screening for abdominal aortic aneurysm: U.S. Preventive Services Task Force recommendation statement. *Ann Intern Med* 2014;161:281–290. [PubMed: 24957320]

2. Behr-Rasmussen C, Grondal N, Bramsen MB, Thomsen MD, Lindholt JS. Mural thrombus and the progression of abdominal aortic aneurysms: A large population-based prospective cohort study. *Eur J Vasc Endovasc Surg* 2014;48:301–307. [PubMed: 24969094]
3. Speelman L, Schurink GW, Bosboom EM, et al. The mechanical role of thrombus on the growth rate of an abdominal aortic aneurysm. *J Vasc Surg* 2010;51:19–26. [PubMed: 19944551]
4. Wolf YG, Thomas WS, Brennan FJ, Goff WG, Sise MJ, Bernstein EF. Computed tomography scanning findings associated with rapid expansion of abdominal aortic aneurysms. *J Vasc Surg* 1994;20:529–535; discussion 535–528. [PubMed: 7933254]
5. Fillinger MF, Marra SP, Raghavan ML, Kennedy FE. Prediction of rupture risk in abdominal aortic aneurysm during observation: Wall stress versus diameter. *J Vasc Surg* 2003;37:724–732. [PubMed: 12663969]
6. Vorp DA, Lee PC, Wang DH, et al. Association of intraluminal thrombus in abdominal aortic aneurysm with local hypoxia and wall weakening. *J Vasc Surg* 2001;34:291–299. [PubMed: 11496282]
7. Haller SJ, Crawford JD, Courchaine KM, et al. Intraluminal thrombus is associated with early rupture of abdominal aortic aneurysm. *J Vasc Surg* 2018;67:1051–1058. [PubMed: 29141786]
8. Stenbaek J, Kalin B, Swedenborg J. Growth of thrombus may be a better predictor of rupture than diameter in patients with abdominal aortic aneurysms. *Eur J Vasc Endovasc Surg* 2000;20:466–469. [PubMed: 11112467]
9. Nguyen VL, Leiner T, Hellenthal FA, et al. Abdominal aortic aneurysms with high thrombus signal intensity on magnetic resonance imaging are associated with high growth rate. *Eur J Vasc Endovasc Surg* 2014;48: 676–684. [PubMed: 24935911]
10. Zhu C, Haraldsson H, Faraji F, et al. Isotropic 3D black blood MRI of abdominal aortic aneurysm wall and intraluminal thrombus. *Magn Reson Imaging* 2016;34:18–25. [PubMed: 26471514]
11. Zhu C, Tian B, Leach JR, et al. Non-contrast 3D black blood MRI for abdominal aortic aneurysm surveillance: Comparison with CT angiography. *Eur Radiol* 2017;27:1787–1794. [PubMed: 27553926]
12. Wang Y, Seguro F, Kao E, et al. Segmentation of lumen and outer wall of abdominal aortic aneurysms from 3D black-blood MRI with a registration based geodesic active contour model. *Med Image Anal* 2017; 40:1–10. [PubMed: 28549310]
13. Zhang X, Zhu C, Peng W, et al. Scan-rescan reproducibility of high resolution magnetic resonance imaging of atherosclerotic plaque in the middle cerebral artery. *PLoS One* 2015;10:e0134913. [PubMed: 26247869]
14. Brady AR, Thompson SG, Fowkes FG, Greenhalgh RM, Powell JT, Participants UKSAT. Abdominal aortic aneurysm expansion: Risk factors and time intervals for surveillance. *Circulation* 2004;110:16–21. [PubMed: 15210603]
15. Vardulaki KA, Prevost TC, Walker NM, et al. Growth rates and risk of rupture of abdominal aortic aneurysms. *Br J Surg* 1998;85:1674–1680. [PubMed: 9876073]
16. Wilson JS, Virag L, Di Achille P, Karsaj I, Humphrey JD. Biochemomechanics of intraluminal thrombus in abdominal aortic aneurysms. *J Biomech Eng* 2013;135:021011. [PubMed: 23445056]
17. Golledge J, Wolanski P, Parr A, Buttner P. Measurement and determinants of infrarenal aortic thrombus volume. *Eur Radiol* 2008;18: 1987–1994. [PubMed: 18414871]
18. Harter LP, Gross BH, Callen PW, Barth RA. Ultrasonic evaluation of abdominal aortic thrombus. *J Ultrasound Med* 1982;1:315–318. [PubMed: 7166768]
19. Arzani A, Suh GY, Dalman RL, Shadden SC. A longitudinal comparison of hemodynamics and intraluminal thrombus deposition in abdominal aortic aneurysms. *Am J Physiol Heart Circ Physiol* 2014;307: H1786–1795. [PubMed: 25326533]
20. Di Achille P, Tellides G, Figueroa CA, Humphrey JD. A haemodynamic predictor of intraluminal thrombus formation in abdominal aortic aneurysms. *Proc R Soc A Math Phys Eng Sci* 2014;470(2172).
21. Thubrikar MJ, Robicsek F, Labrosse M, Chervenkov V, Fowler BL. Effect of thrombus on abdominal aortic aneurysm wall dilation and stress. *J Cardiovasc Surg* 2003;44:67–77. [PubMed: 12627076]

22. Di Martino ES, Vorp DA. Effect of variation in intraluminal thrombus constitutive properties on abdominal aortic aneurysm wall stress. *Ann Biomed Eng* 2003;31:804–809. [PubMed: 12971613]
23. Martufi G, Lindquist Liljeqvist M, Sakalihasan N, et al. Local diameter, wall stress, and thrombus thickness influence the local growth of abdominal aortic aneurysms. *J Endovasc Ther* 2016;23:957–966. [PubMed: 27412646]
24. Shi Z, Zhu C, Degnan AJ, et al. Identification of high-risk plaque features in intracranial atherosclerosis: Initial experience using a radiomic approach. *Eur Radiol* 2018;28:3912–3921. [PubMed: 29633002]
25. Reeps C, Essler M, Pelisek J, Seidl S, Eckstein HH, Krause BJ. Increased 18F-fluorodeoxyglucose uptake in abdominal aortic aneurysms in positron emission/computed tomography is associated with inflammation, aortic wall instability, and acute symptoms. *J Vasc Surg* 2008;48: 417–423; discussion 424. [PubMed: 18572354]
26. Hope MD, Hope TA. Functional and molecular imaging techniques in aortic aneurysm disease. *Curr Opin Cardiol* 2013;28:609–618. [PubMed: 24030165]
27. Richards JM, Semple SI, MacGillivray TJ, et al. Abdominal aortic aneurysm growth predicted by uptake of ultrasmall superparamagnetic particles of iron oxide: A pilot study. *Circ Cardiovasc Imaging* 2011;4: 274–281. [PubMed: 21304070]
28. Conlisk N, Forsythe RO, Hollis L, et al. Exploring the biological and mechanical properties of abdominal aortic aneurysms using USPIO MRI and peak tissue stress: A combined clinical and finite element study. *J Cardiovasc Transl Res* 2017 [Epub ahead of print].
29. Castrucci M, Mellone R, Vanzulli A, et al. Mural thrombi in abdominal aortic aneurysms: MR imaging characterization—Useful before endovascular treatment? *Radiology* 1995;197:135–139. [PubMed: 7568811]

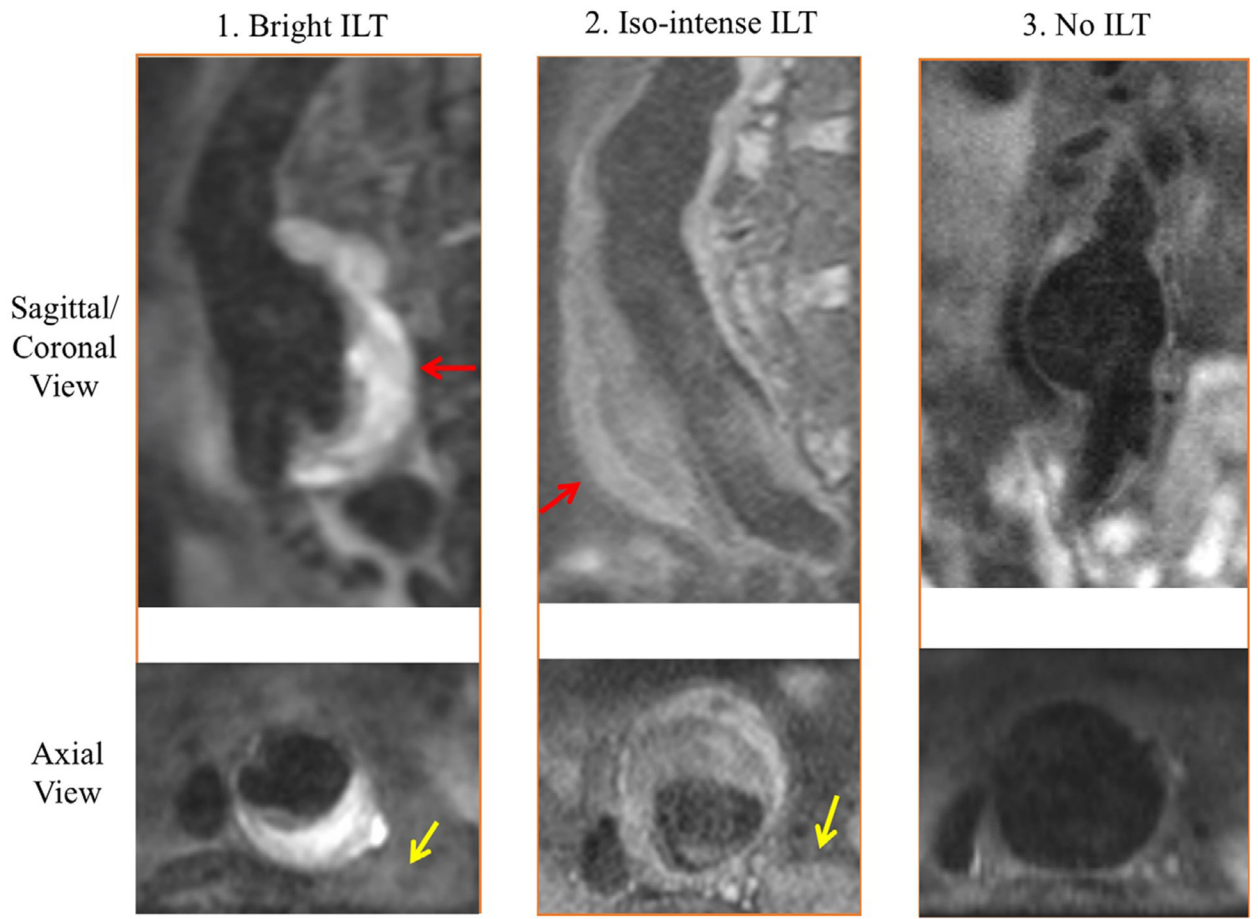


FIGURE 1: Different ILT types shown on black-blood MRI. Red arrows show the ILT. Yellow arrows show the psoas muscle.

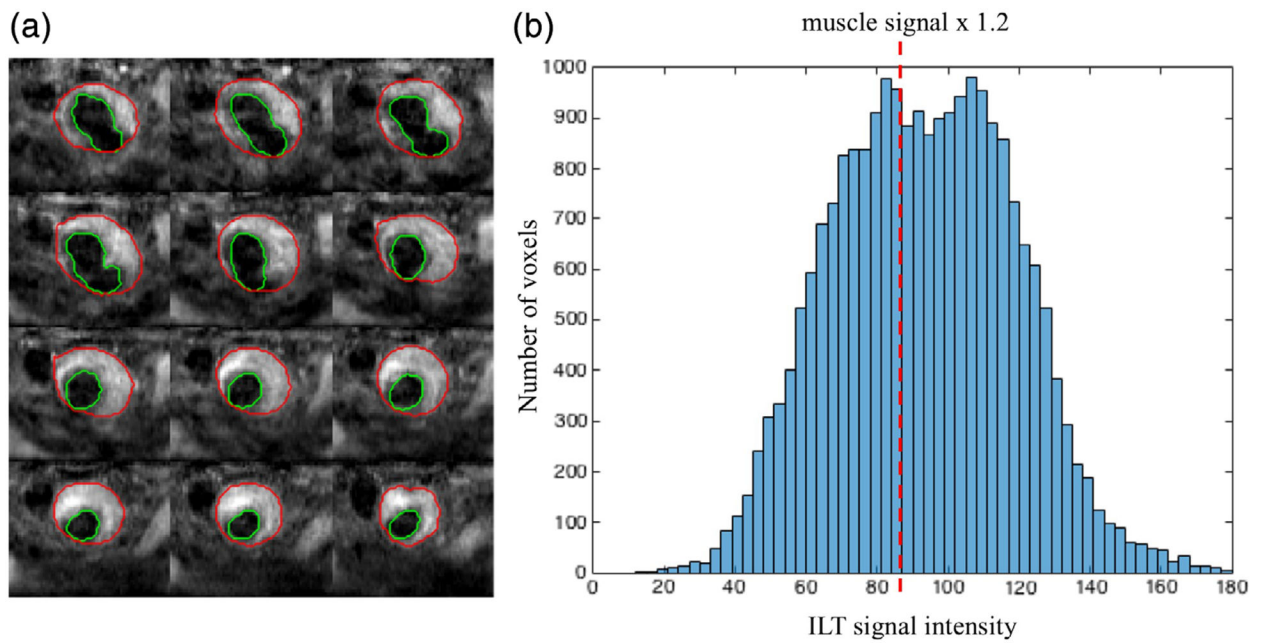


FIGURE 2:

Automatic segmentation of ILT and signal intensity histogram. **(a)** Examples of automatic segmentation of lumen and outer wall boundaries (one slice of every four slices is shown). **(b)** ILT signal intensity histogram. Red dash line shows the 1.2 times of muscle signal. This AAA has mostly bright ILT.

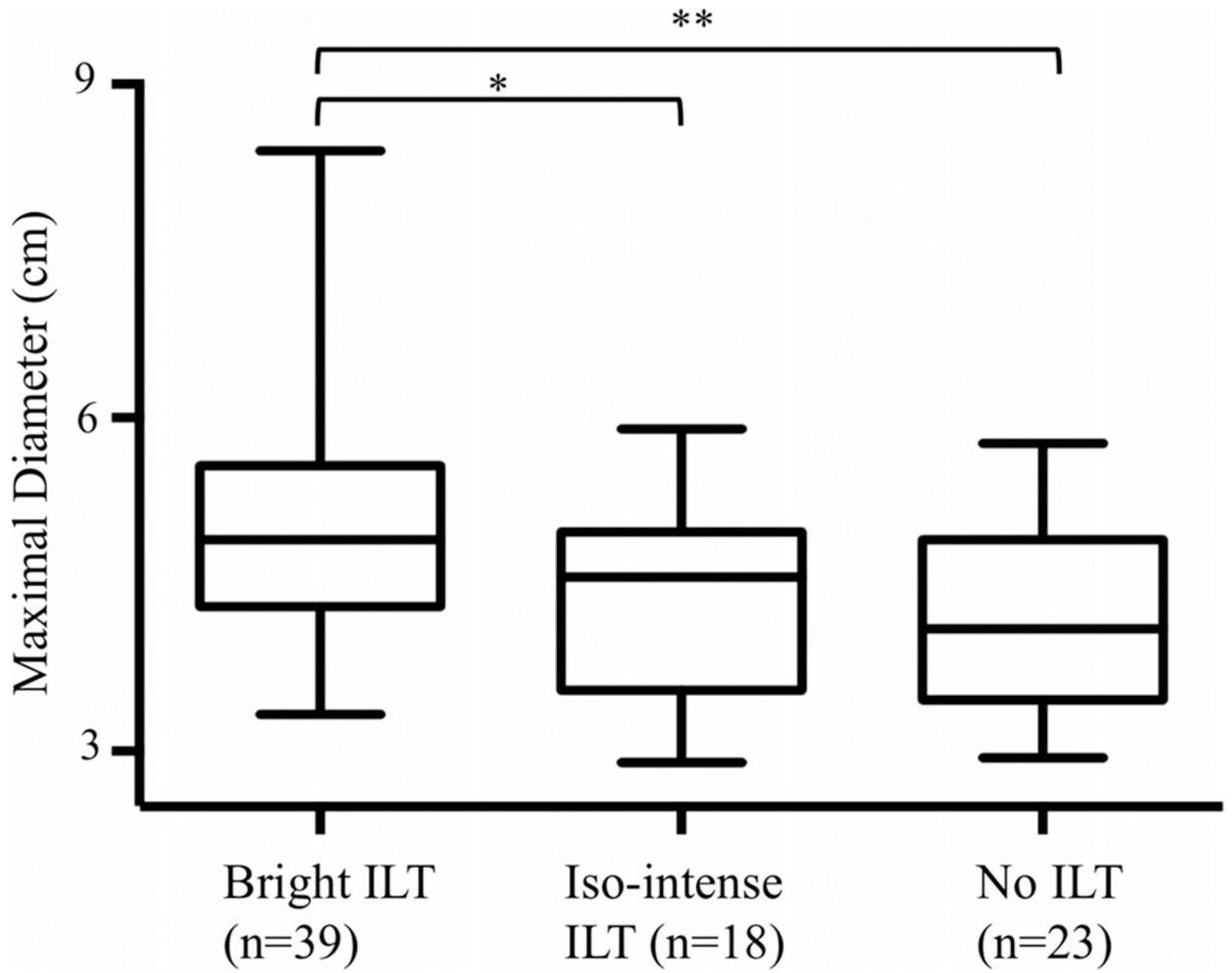


FIGURE 3: Diameters of three AAA types. AAAs with bright ILT are larger than AAAs with iso-intense ILT or no ILT (5.1 ± 1.1 cm, 4.4 ± 0.9 cm, 4.2 ± 0.8 cm, $P = 0.008$). No significant difference was found between iso-intense ILT and no ILT groups ($P = 0.49$).

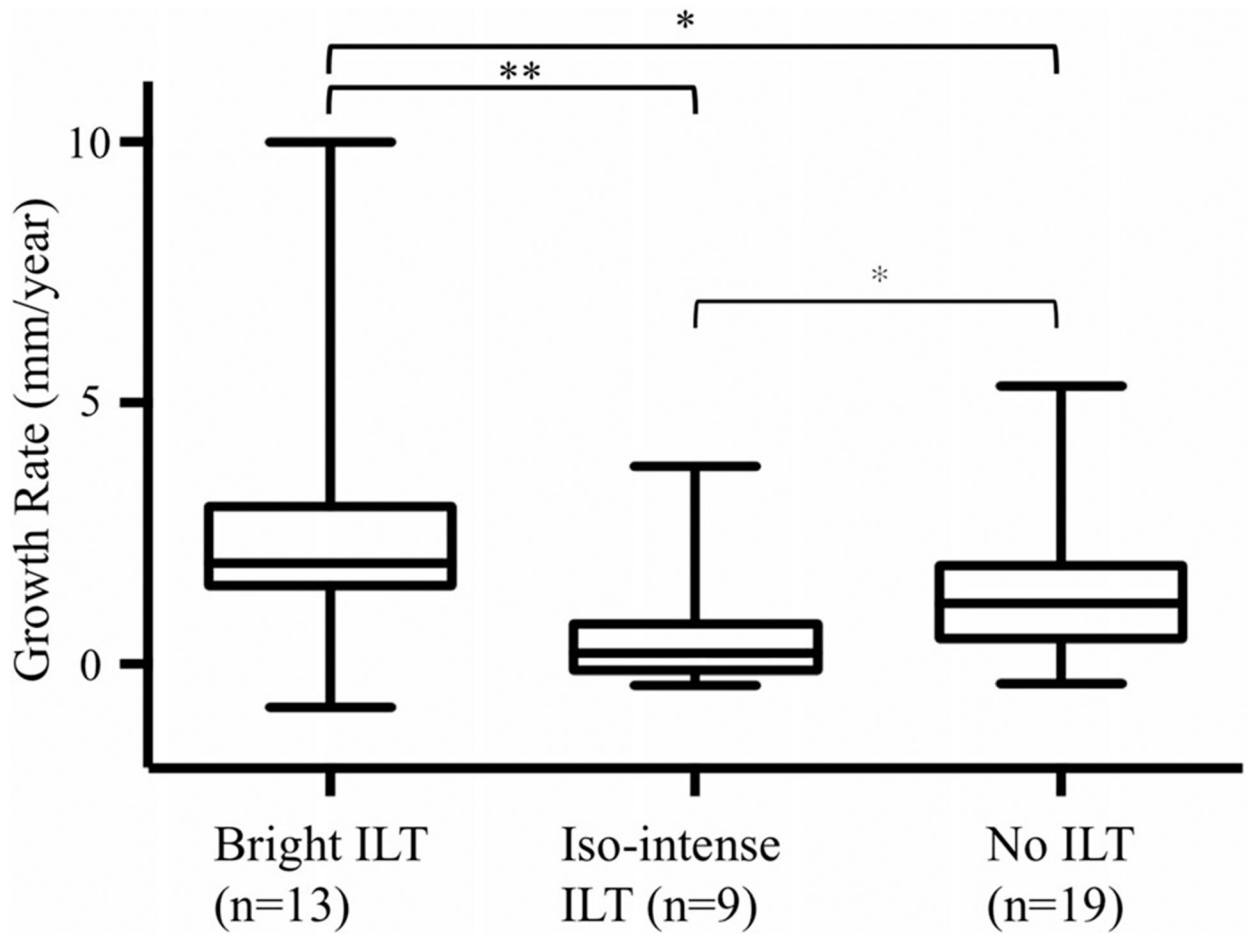


FIGURE 4:

Growth rate of three types of AAAs. The growth rate of AAA with bright ILT is significantly higher than AAAs with isointense ILT or no ILT (2.6 ± 2.5 , 0.6 ± 1.3 , 1.5 ± 1.6 mm/year, $P = 0.01$). * $P < 0.05$; ** $P < 0.01$.

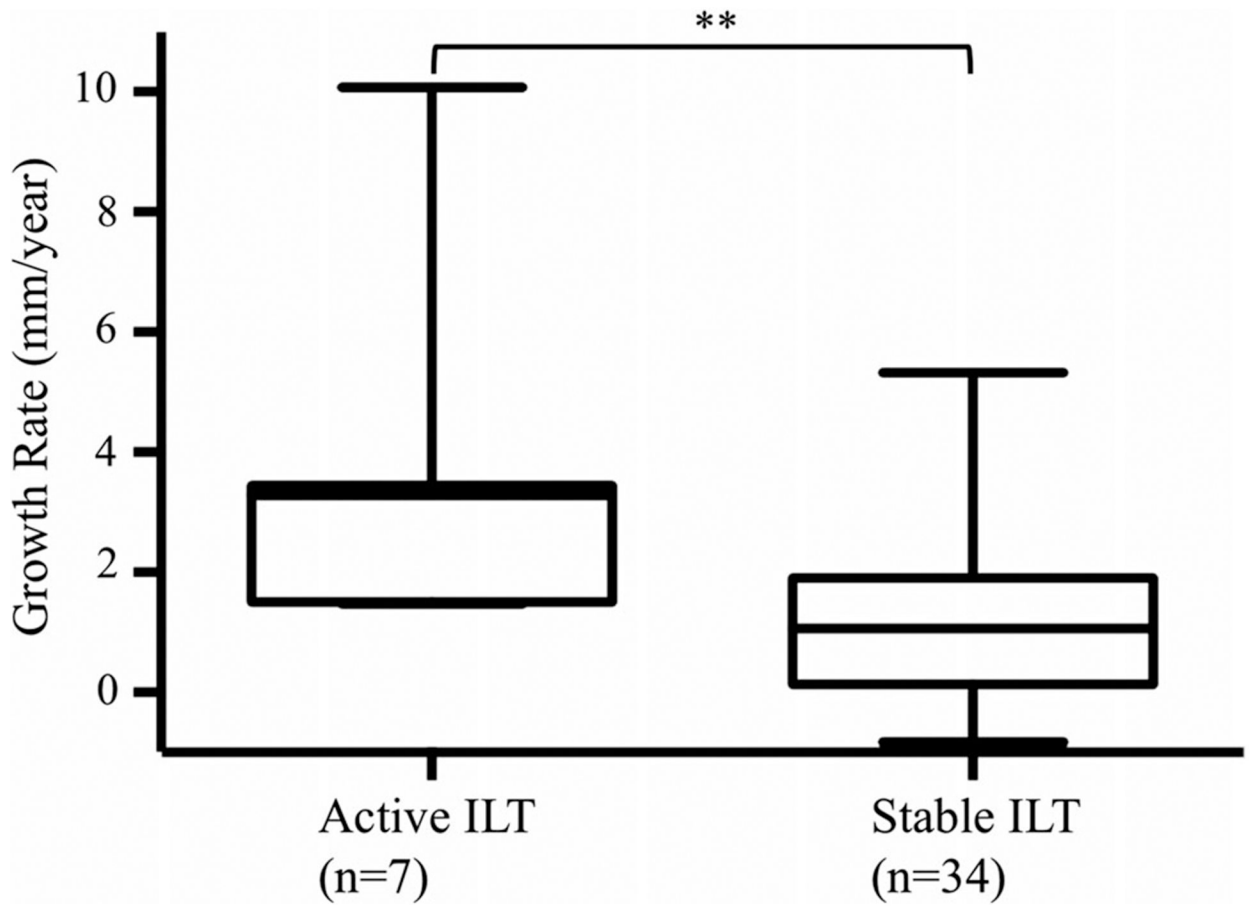


FIGURE 5:

AAAs with active ILT change has a significantly higher growth rate than AAAs with stable ILT (3.6 ± 3.0 mm/year vs. 1.2 ± 1.3 mm/year, $P = 0.008$). * $P < 0.05$; ** $P < 0.01$.

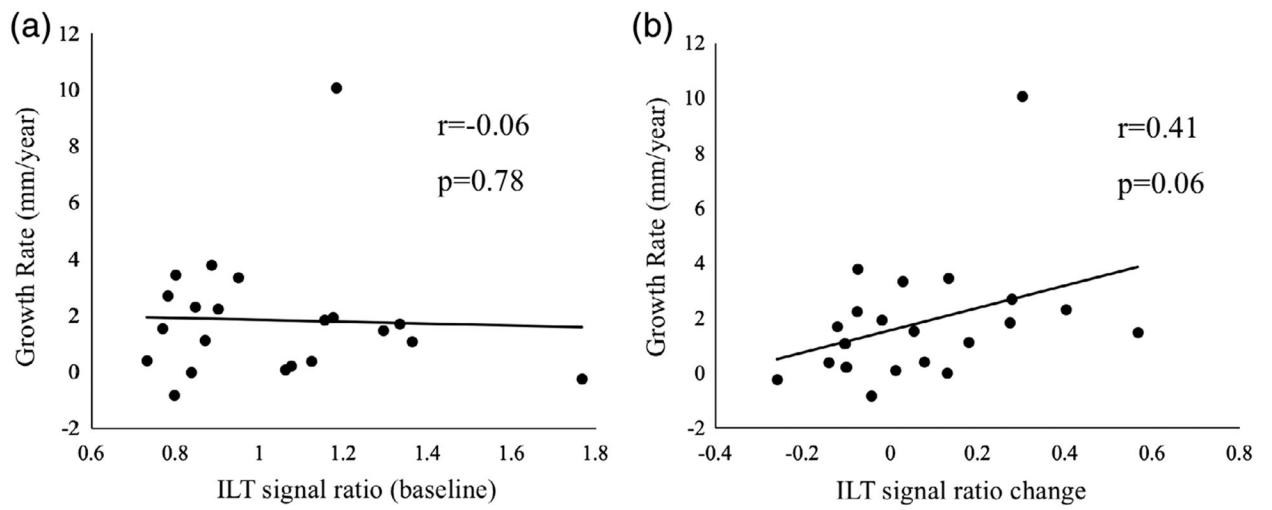


FIGURE 6:
Relationship between baseline ILT-to-muscle signal ratio/change overtime with AAA growth.

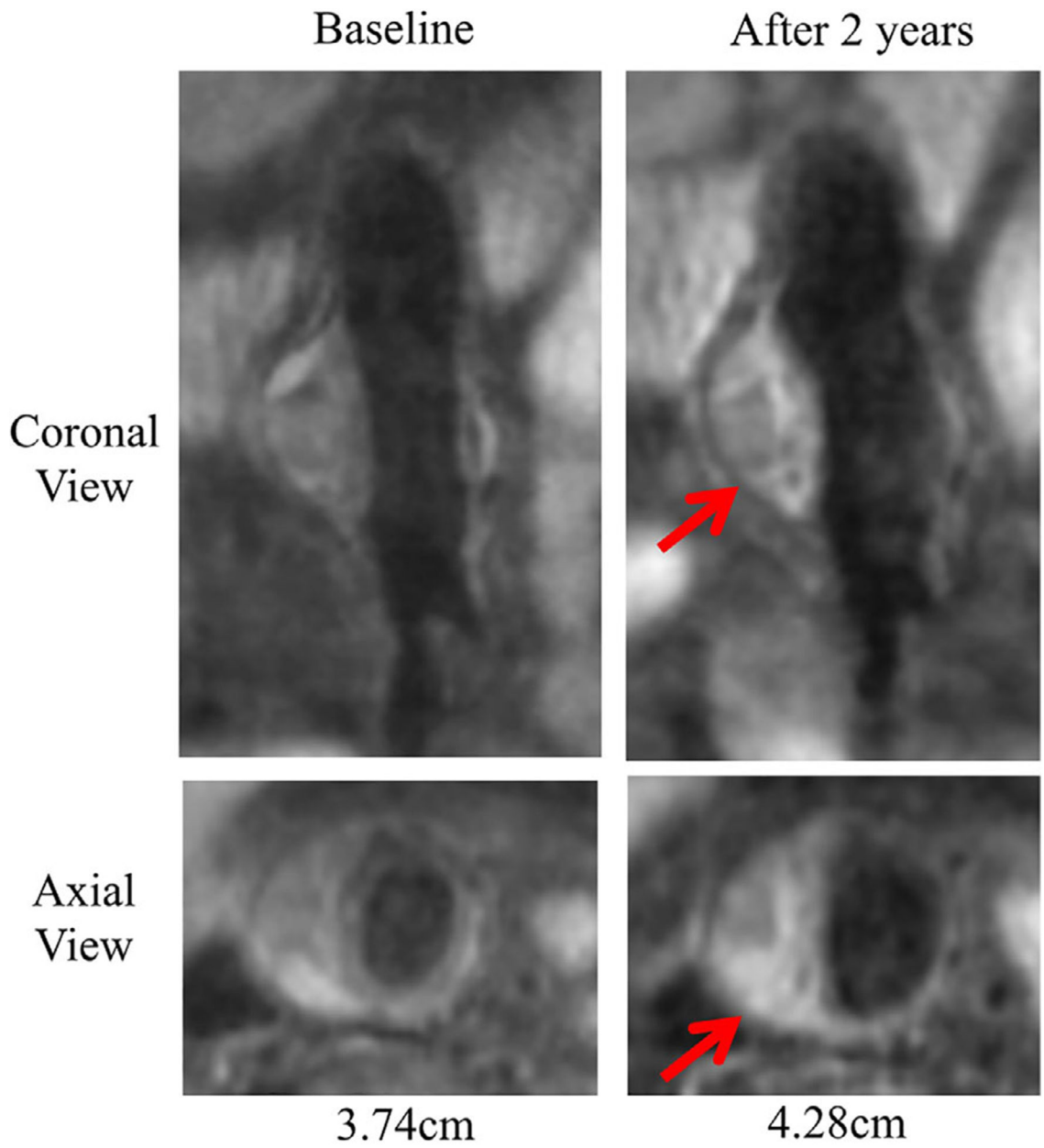


FIGURE 7: Bright ILT predicts AAA fast growing (2.7 mm/year). ILT became brighter in 2 years' time. ILT also grew towards the lumen, and slightly changed the lumen shape. Red arrows show the ILT.

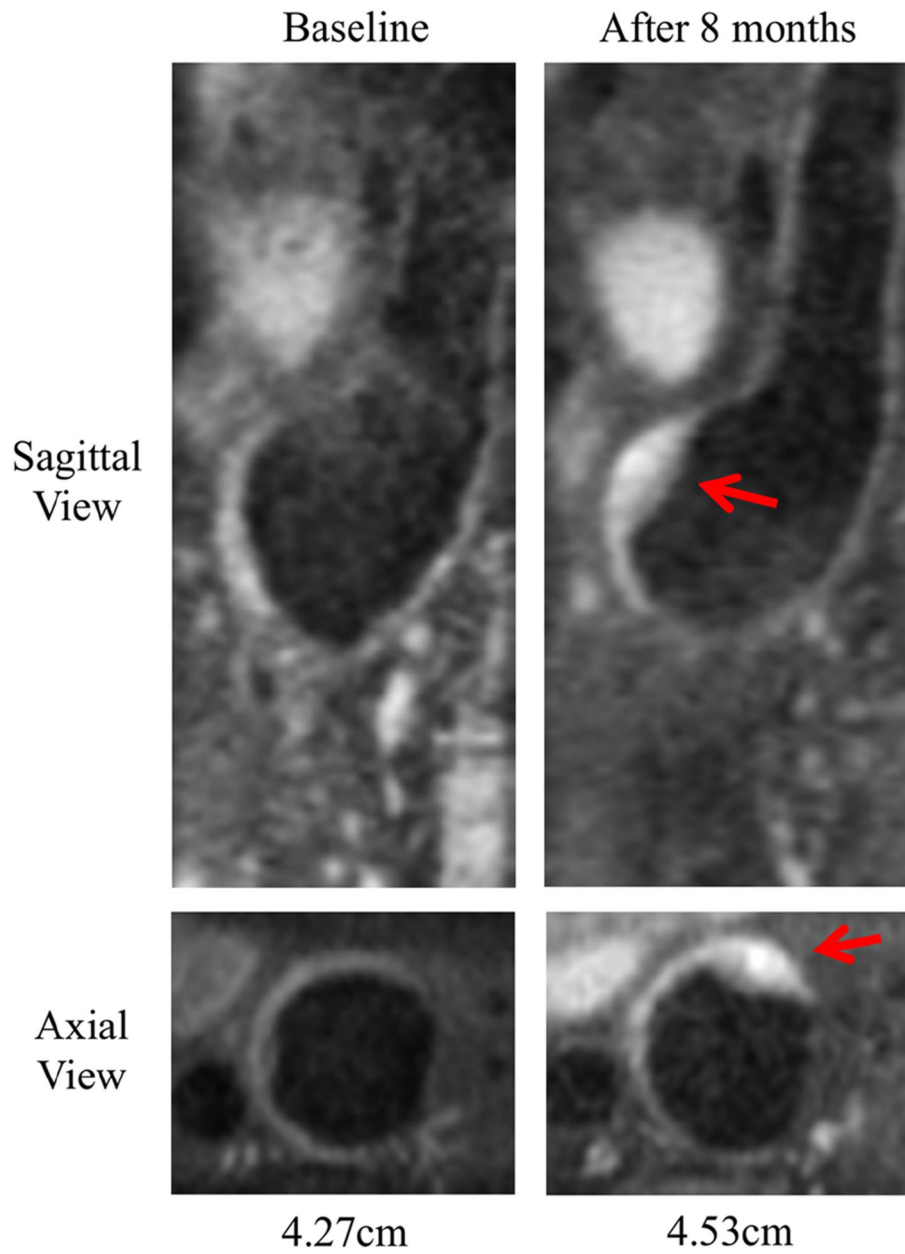


FIGURE 8: An AAA with new ILT formation during follow-up (growth rate 3.5 mm/year). There was no ILT at baseline. After 8 months, a new, thin, bright ILT appeared in the anterior part of the aneurysm.

TABLE 1.

Patient Demographics

	All (n = 80)	Bright ILT (n = 39)	Isointense ILT (n = 18)	No ILT (n = 23)	P-value
Age (y), mean \pm SD	72 \pm 7	73 \pm 7	71 \pm 7	73 \pm 8	0.43
Male, n, %	75 (93.8)	38 (97.4)	15 (83.3)	22 (95.7)	0.13
Hypertension, ^a n, %	59 (73.8)	28 (71.8)	13 (72.2)	18 (78.3)	0.89
DM, ^b n, %	19 (23.8)	10 (25.6)	4 (22.2)	5 (21.7)	0.94
Smoking, ^c n, %	46 (57.5)	18 (46.2)	13 (72.2)	15 (65.2)	0.13
CAD, ^c n, %	30 (37.5)	14 (35.9)	9 (50)	7 (30.4)	0.45

^aHypertension is defined as resting blood pressure > 140/90 mmHg.

^bDiabetes mellitus.

^cCoronary artery disease.